

Feshbach resonances in ultracold atom-molecule collisions

Andrea Simoni and Jean-Michel Launay

Institut de Physique de Rennes, CNRS and Université de Rennes 1, UMR 6251, 35042 Rennes Cedex, France

Pavel Soldán

Department of Chemical Physics and Optics, Faculty of Mathematics and Physics, Charles University in Prague, Ke Karlovu 3, 121 16 Prague 2, Czech Republic

(Received 7 December 2008; published 3 March 2009)

We investigate the presence of Feshbach resonances in ultracold alkali-dialkali reactive collisions. A potential-energy surface of Na_3 in the lowest quartet state is constructed and used in quantum scattering calculations. An analysis of scattering features is performed through a systematic variation in the nonadditive three-body interaction potential. Our results should provide useful information for interpreting future atom-molecule collision experiments.

DOI: [10.1103/PhysRevA.79.032701](https://doi.org/10.1103/PhysRevA.79.032701)

PACS number(s): 34.50.Cx, 31.50.Bc

I. INTRODUCTION

In recent years, there has been a growing interest in ultracold molecules [1], particularly in the production and properties of the molecules formed from ultracold atomic gases [2]. Photoassociation [3] and Feshbach resonance tuning [4] are two main experimental techniques for a coherent production of ultracold molecules from ultracold alkali-metal atoms. In 2003 long-lived molecular Bose-Einstein condensates were created from weakly bound homonuclear lithium and potassium dimers by exploiting magnetically tunable Feshbach resonances between fermionic isotopes [5–7].

While Feshbach resonances are always located at the highest vibrational manifold of the dimer, photoassociation could in principle allow access to low vibrational dimer states. In 2005 RbCs molecules were created in their ground vibronic state [8]. Very recently, several different photoassociation schemes for molecular formation in the ground vibronic state have also been developed [9–13].

For the correct interpretation of the forthcoming experiments with cold molecular samples it is essential to understand the atom-molecule and molecule-molecule interactions at sub-K temperatures [14]. Theoretical results have already been published for the homonuclear $X+X_2$ ultralow-energy collisions with $X=\text{Li}$, Na , and K [15–20]. Isotopically heteronuclear $\text{Li}+\text{Li}_2$ ultralow-energy collisions have also been studied theoretically [20–24]. Collision cross sections have been measured experimentally for the $\text{Cs}+\text{Cs}_2$ ultracold inelastic processes [25,26]. Very recently reactive and inelastic rate constants were measured for $\text{Li}+\text{Li}_2^*$ at room temperature [27].

Cold collisions are known to be very sensitive to potential-energy surfaces [16,20], and therefore experimental information is needed to improve the corresponding theoretical models. In particular, knowledge of low-energy resonance patterns often allows different properties of the interaction potential to be determined with high accuracy. Such resonances have been studied in great detail both theoretically and experimentally in ultracold atomic gases; see, e.g., [28–30].

On the other hand, very little is known about atom-molecule resonances in ultracold collisions. Similarly to

atomic scattering the hyperfine-induced resonances could in principle exist at very low collision energies. However, model calculations have shown that for a general polarization they will be quenched by inelastic spin-exchange transitions forming singlet molecules [31].

Alkali-metal dimers on the lowest electronic triplet manifold are only stable if they are in a doubly spin-polarized state under collisions with doubly spin-polarized atoms (assuming that the relativistic spin interactions are neglected). Unfortunately, for this specific polarization hyperfine-induced resonances are prevented by symmetry (resonances induced by relativistic spin interactions are still possible). In spite of this, long-lived three-atom complexes can in principle exist and give rise to resonances. Such reactive resonances have been identified in reactive collisions at room temperature [32].

In this work, we focus on collisions of Na_2 molecules in the triplet electronic state with ground-state Na atoms. For this study a potential-energy surface of $\text{Na}_3(1^4A'_2)$ has been constructed. The occurrence of long-lived three-atom resonances in such collision complex is demonstrated in the ultracold regime. We also study the dependence of collision cross sections on the potential-energy surface and we show that at least knowledge of two terms in the cross-section partial-wave expansion is needed in order to characterize further the three-body potential.

II. POTENTIAL ENERGY SURFACE

Ab initio calculations were performed using a single-reference restricted open-shell variant [33] of the coupled-cluster method [34] with single, double, and noniterative triple excitations [RCCSD(T)]. A basis set consisting of (12s, 12p, 5d, 2f, 1g) basis functions [35] was used for the dimer calculations, and the same basis set without the *g* functions was used for the trimer calculations. Electrons from the 1s orbital on each sodium atom were not correlated in the coupled-cluster calculations. The three-atom interaction potential was decomposed into a sum of pairwise additive and nonadditive contributions,

$$V_{\text{trimer}}(r_{12}, r_{23}, r_{13}) = \sum_{i<j} V_{\text{dimer}}(r_{ij}) + V_3(r_{12}, r_{23}, r_{13}). \quad (1)$$

It has been shown by several authors that in the case of alkali-metal trimers the nonadditive term $V_3(r_{12}, r_{23}, r_{13})$ is rather large and cannot be neglected [36–38]. Interaction energies were calculated with respect to the separated-atom dissociation limit, and the full counterpoise correction of Boys and Bernardi [39] was employed to compensate for the basis set superposition error in both the dimer and trimer calculations. All the *ab initio* calculations were performed using the MOLPRO quantum chemistry package [40].

Forty-seven dimer interaction energies V_{dimer} on the $a^3\Sigma_u^+$ manifold were calculated on an irregular grid covering the range of interatomic distances from 2.0 to 14.0 Å. These points were interpolated using the one-dimensional (1D) reciprocal-power reproducing kernel Hilbert-space (RP-RKHS) method [41]. The interpolation was done with respect to r^2 using RP-RKHS parameters ($m=2$ and $n=3$). The resulting curve had a minimum at approximately $r_e = 5.194$ Å, $V_{\text{dimer}}(r_e) = -172.946$ cm⁻¹, which is slightly higher than the previously reported *ab initio* minima $r_e = 5.192$ Å, $V_{\text{dimer}}(r_e) = -177.7$ cm⁻¹ [42], $r_e = 5.20$ Å, $V_{\text{dimer}}(r_e) = -176.17$ cm⁻¹ [36], and $r_e = 5.214$ Å, $V_{\text{dimer}}(r_e) = -174.025$ cm⁻¹ [37].

Ivanov *et al.* [43] analyzed experimental data on triplet Na₂ and derived the accurate position $r_e = 5.166\,07$ Å, $V_{\text{dimer}}(r_e) = -173.649\,60$ cm⁻¹ of the $a^3\Sigma_u^+$ minimum. Therefore our *ab initio* interaction energies were shifted and scaled (shifted by $-0.027\,54$ Å and scaled by $1.004\,07$) so that the minimum of the modified potential-energy curve coincided with the minimum determined from experiment. The RP-RKHS interpolation was then repeated using the modified RP-RKHS method [44]. Beyond the last *ab initio* point, the potential energy was then extrapolated to the form

$$V_{\text{dimer}}(r) = -\frac{C_6}{r^6} - \frac{C_8}{r^8} - \frac{C_{10}}{r^{10}}. \quad (2)$$

The long-range coefficients C_6 and C_8 were kept fixed to the values of $1.561 \times 10^3 E_h a_0^6$ and $1.16 \times 10^5 E_h a_0^8$, respectively [45]. The value of the “free” long-range coefficient C_{10} was then determined from the corresponding RP-RKHS coefficients [46] to be $1.19 \times 10^7 E_h a_0^{10}$, which compares very well with $1.158 \times 10^7 E_h a_0^{10}$ from Ref. [45]. The resulting potential-energy curve supports 16 vibrational bound states and gives a scattering length of $67.1a_0$, which compares reasonably well (within 10%) with published values 65.3 [47], 63.9 [48], and 62.51 [49].

Three hundred fifty-six trimer interaction energies V_{trimer} on the $1^4A_2'$ manifold were calculated on a regular three-dimensional (3D) grid covering the range of interatomic distances from 2.5 to 10.0 Å (geometry configurations were unique up to a permutation of atoms and satisfied the triangular inequality $|r_{12} - r_{13}| \leq r_{23} \leq r_{12} + r_{13}$; at linear geometries, where $r_{23} = r_{12} + r_{13}$, the distance r_{23} was permitted to extend beyond 10.0 Å).

The grid consisted of 220 C_{2v} points (including 16 D_{3h} points) and 136 $C_{\infty v}$ points (including 16 $D_{\infty h}$ points). From the trimer interaction energies the counterpoise corrected

nonadditive energies V_3 were extracted using Eq. (1).

The nonadditive energy function V_3 was represented in the same manner as in the case of the spin-polarized potassium trimer [18,50]. In order to accommodate the geometric dependencies of the long-range multipole terms, third-order dipole-dipole-dipole [51] and dipole-dipole-quadrupole [52] terms were subtracted from the nonadditive energy V_3 . Their corresponding long-range coefficients C_9 and C_{11} were fixed to $1.892 \times 10^5 E_h a_0^9$ [45] and $1.468\,12 \times 10^5 E_h a_0^{11}$, respectively [53]. The leading term of the remaining multipole asymptotic expansion was the fourth-order dipole-dipole-dipole term [54], and after a multiplication by a suitable function it was prepared for an “isotropic” extrapolation [18,50]. The resulting points were then interpolated, using the fully symmetrized 3D RP-RKHS interpolation method [36], in each interatomic distance with respect to the reduced coordinate $\rho = (\frac{r}{S})^3$ and with RP-RKHS parameters $S = 10.0$ Å, $m = 0$, and $n = 2$.

The three-atom interaction potential V_{trimer} for the $1^4A_2'$ state of Na₃ was then reconstructed using Eq. (1). Its D_{3h} global minimum of -880.9 cm⁻¹ is at $r_{12} = r_{13} = r_{23} = 4.34$ Å and $D_{\infty h}$ saddle point of -381.7 cm⁻¹ is at $r_{12} = r_{13} = 5.06$ Å. The minimum of our trimer potential is approximately 5% deeper than the minima reported by Higgins *et al.* [36] and Soldán *et al.* [37]. Two cuts through the surface are shown as contour plots in Fig. 1 for values of the valence angles 60° and 180° .

III. QUANTUM DYNAMICS

The scattering observables are obtained by solving the time-independent Schrödinger equation for three atoms. Quantum dynamical calculation is performed using hyperspherical democratic coordinates. This system of coordinates is comprised of three internal coordinates (two hyperangles and one hyper-radius) describing the shape and the size of the molecular triangle and three Euler angles describing the orientation of the molecular plane in space. The total wave function is expanded on a set of hyperspherical basis functions varying with the hyper-radius. The resulting closed coupled equations are solved using a logarithmic-derivative propagator approach. Details on the method can be found in [55].

The hyperspherical democratic coordinates are especially well adapted in describing alkali-metal species reactions that mainly proceed through an insertion mechanism [15]. However, the region of large interparticle distances, where the system separates into atom and molecule, is not efficiently described in hyperspherical coordinates. Therefore the scattering wave function in the outer region is computed using Jacobi coordinates. State-to-state probability amplitudes are finally extracted by matching to the short-range wave function obtained with the hyperspherical approach [55].

Atom-atom collisions in the ultracold regime are determined by a small number of parameters. In fact, the s -wave scattering lengths and the dominant term in the long-range multipole potential expansion are sufficient in general to predict all near-threshold scattering and bound-state properties. This feature has allowed many systems of experimental in-

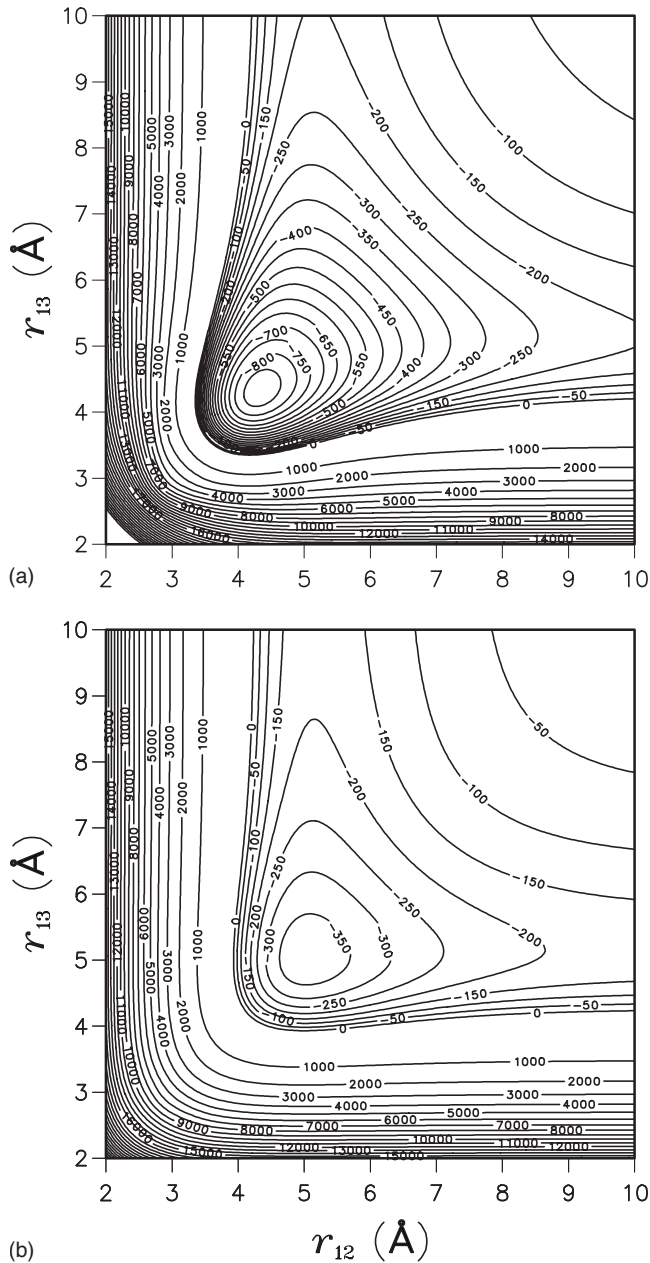


FIG. 1. Cuts through the Na_3 quartet surface in valence coordinates. Upper panel: cut for a bond angle of 60° ; the global minimum of -881 cm^{-1} is at $r_{12}=r_{13}=r_{23}=4.34 \text{ \AA}$. Lower panel: cut at collinear geometries; the collinear minimum of -382 cm^{-1} is at $r_{12}=r_{13}=5.06 \text{ \AA}$. Contours are labeled in cm^{-1} .

interest to be accurately modeled based on a limited amount of experimental information [28–30]. Observed energy-dependent cross sections and Feshbach or shape resonances often provided a key piece of information for determining theoretically the scattering lengths and the long-range dispersion coefficients.

The situation appears to be more complex for atom-molecule collisions due to the additional rovibrational degrees of freedom and anisotropic interactions. As collisional data may be soon available we begin to study here what experimental information might be best suited to constrain the collision models. For most alkali-metal systems, and for

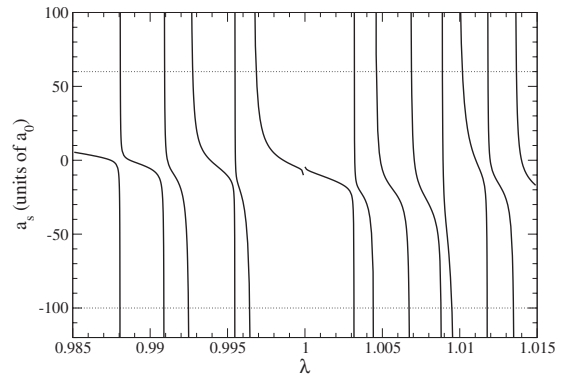


FIG. 2. The $\text{Na}+\text{Na}_2$ ($v=0, j=0$) s -wave scattering length as a function of the three-body control parameter λ (see text). Horizontal lines identify model potentials corresponding to $a_s=-100a_0$ and $60a_0$.

Na_2 in particular, the two-body potential is known with high accuracy from a combination of conventional room temperature and ultracold atom spectroscopy [49]. Therefore, one may expect the three-body interaction V_3 to represent the largest source of uncertainty. We assume that its shape is essentially correct and following the approach of [16], we solve the scattering problem with a scaled potential λV_3 . At variance with Ref. [16] which considered inelastic scattering we discuss here scattering resonances in elastic collisions.

We focus on molecules in the lowest triplet rovibrational state, which is collisionally stable under two-body collisions with atoms if both colliding partners have maximal spin projection on the quantization axis. We show in Fig. 2 the atom-diatom s -wave scattering length a_s as a function of the three-body control parameter λ . Each time a three-body bound state crosses the dissociation threshold the a_s presents a typical divergence, termed a zero-energy resonance. One may note that a 0.1–1% potential variation ($1\text{--}10 \text{ cm}^{-1}$ on the potential depth) is sufficient for a complete $-\infty$ to $+\infty$ variation in a_s .

In order to investigate the relation between the zero-energy quantity a_s and finite-energy scattering, we select values of the control parameter λ corresponding to the same value of a_s and compare the corresponding energy-dependent elastic cross sections.

We first consider total angular momentum $J=0$. For $j=0$ rotational states this implies an angular momentum $\ell=0$. Figure 3 shows the result of the comparison for a typical positive value of a_s . The partial $J=0$ cross sections σ for $a_s > 0$ show a qualitatively similar behavior essentially determined by the value of a_s and by the long-range C_6 coefficient. One can remark the well-known zero-energy limit $\sigma \rightarrow 4\pi a_s^2$. The minimum of the cross section corresponds to the scattering phase shift going through a multiple of π , and in the absence of contributions from higher order partial waves would correspond to a Ramsauer-Townsend minimum in the total cross section [56].

The cross sections calculated for $a_s < 0$ are more interesting. A large negative scattering length is associated with a bound state turned into a virtual state with energy E_0 in the continuum. This situation can be conveniently described by decomposing the elastic phase shift into a background plus a resonance contribution [56,57],

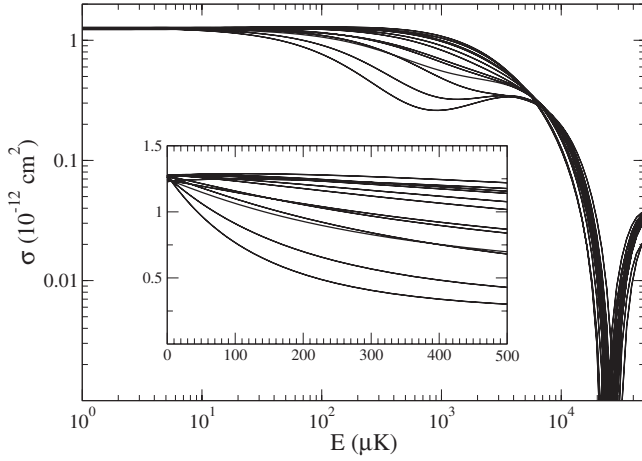


FIG. 3. The partial $J=0$ $\text{Na}+\text{Na}_2$ ($v=0, j=0$) elastic cross section as a function of collision energy for different values of the three-body control parameter determined by the same value of the atom-diatom scattering length $a_s=60a_0$. The inset refers to the typical energy regime of current ultracold molecule experiments.

$$\delta = \delta_{\text{bg}} + \delta_{\text{res}}, \quad \delta_{\text{res}} = -\arctan \frac{\gamma/2}{E - E_r}, \quad (3)$$

where $E_r = E_0 + \eta$ is the resonance position, with γ and η as the resonance width and shift, respectively. For the first few angular momenta ℓ low-energy scattering is determined by the asymptotic behavior $\gamma \sim E^{\ell+1/2}$, $\delta_{\text{bg}} \sim E^{\ell+1/2}$, and $\eta \sim \text{const}$ [57].

There will be a low-energy resonance only if the width is sufficiently narrow, $\gamma(E) < E$. If the more strict condition $\gamma(E) \ll E$ is fulfilled, $\gamma(E)$ can be replaced with the constant quantity $\gamma_r = \gamma(E_r)$, and the decomposition in Eq. (3) implies that δ undergoes a rapid π variation across resonance. Note that because of the $\gamma \sim E^{1/2}$ threshold law, $\ell=0$ scattering at sufficiently low energy always violates the $\gamma < E$ condition and no resonant behavior will arise. However, this does not rule out the presence of resonances at higher yet very low collision energy (see below).

Resonances can also be analyzed in terms of the Wigner time delay [58],

$$Q = 2\hbar \frac{d\delta}{dE}, \quad (4)$$

i.e., the average delay of a scattering event compared to free transit in the absence of the potential. In the threshold regime using Eq. (3) one obtains

$$Q = \frac{\hbar\gamma}{(E - E_r)^2 + \frac{\gamma^2}{4}} \left(1 - \frac{d\eta}{dE} \right) + \frac{2}{v} \frac{d\delta_{\text{bg}}}{dk} - \frac{E - E_r}{(E - E_r)^2 + \frac{\gamma^2}{4}} \frac{1}{v} \frac{d\gamma}{dk}, \quad (5)$$

where v is the velocity in the relative motion and k is the relative wave vector. The first term is the usual Lorentzian profile arising from exponential decay with a $\frac{d\eta}{dE}$ correction. Near isolated resonances at high energy this is usually the dominant contribution to the time delay; see, e.g., [59]. The

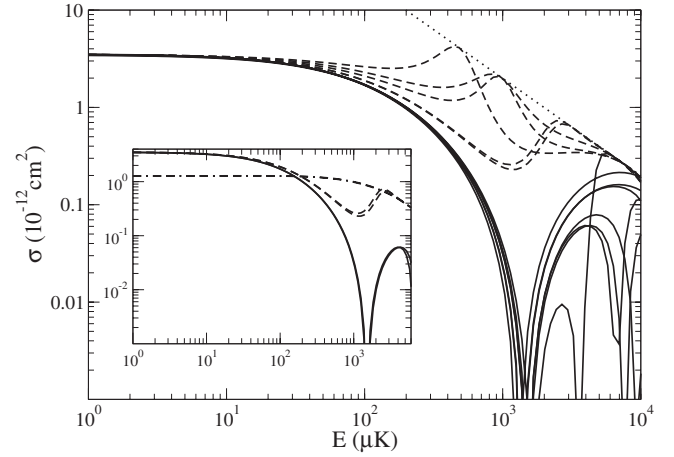


FIG. 4. The partial $J=0$ $\text{Na}+\text{Na}_2$ ($v=0, j=0$) elastic cross section as a function of collision energy for different values of the three-body control parameter determined by the same value of the atom-diatom scattering length $a_s = -100a_0$. Cross sections presenting resonant behavior are identified by dashed lines. The dotted line denotes the unitarity limit (see text). Sample cross sections obtained using different λ and presenting very similar energy dependence are emphasized in the inset. The inset also shows (dashed-dotted lines) two virtually identical cross sections for $a_s > 0$ extracted from Fig. 3.

resonance shift η is usually a slowly varying function of energy but in the presence of additional scattering features such as shape resonances in the background continuum [60].

The second term in Eq. (5) is the classical time for the relative particle to span a distance $2\frac{d\delta_{\text{bg}}}{dk}$. For $\ell=0$ elastic scattering $\delta_{\text{bg}} \sim -ka_{\text{bg}}$, and this term reduces to $-2a_{\text{bg}}/v$ corresponding to an attractive (repulsive) character of the background potential for negative (positive) background scattering lengths a_{bg} . The third term vanishes for $E = E_r$ and gives a correction of dispersive shape across resonance.

Note that in Fig. 4 one can essentially identify two classes of curves. The first class (full lines) presents a monotonically decreasing behavior toward the first minimum, which corresponds to nonresonant scattering. The second class (dashed lines) presents peaks at which the scattering partial cross section reaches the unitarity limit $\sigma = \frac{4\pi}{k^2}$ (dotted line in Fig. 3) and can in principle be associated with a resonant behavior.

We focus on the lowest-energy peak of Fig. 4 and make the three-body potential slightly more attractive in order to further shift this feature toward threshold. Figure 5 shows the $\sin^2 \delta$ and Q quantities for three selected potentials. The feature near 400 μK can be essentially classified as a resonance with $\gamma_r \approx 0.5E_r$. As the potential becomes more binding γ becomes larger than E_r ($\gamma_r = E_r$ for $E_r \approx 200 \mu\text{K}$) and the resonant behavior tends to disappear. As the peak is made to shift closer to threshold the time delay is fully dominated by the background contribution; see upper panel. Also note (lower panel) that in all cases the unitarity limit $\sin^2 \delta = 1$ is attained.

An additional interesting feature that can be observed by inspection of Figs. 3 and 4 is the near coincidence of $J=0$ elastic cross sections computed with different three-body po-

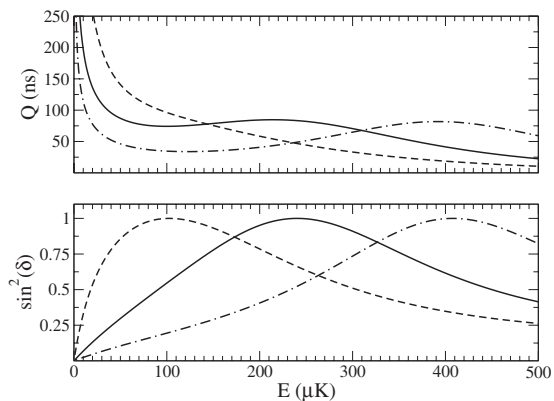


FIG. 5. The Wigner time delay Q (upper panel) and the $\sin^2 \delta$ quantity for $J=0$ $\text{Na}+\text{Na}_2$ ($v=0, j=0$) elastic collisions and selected λ values. Only the peak near $400 \mu\text{K}$ can be classified as a resonance (see text).

tentials in the whole energy range $E < 10$ mK. Sample cross sections illustrating this circumstance for both $a_s > 0$ and $a_s < 0$ are put forth in the inset of Fig. 4. This shows that knowledge of energy-dependent cross sections in the regime where only the $J=0$ partial wave is important is in general not sufficient to determine the strength of the three-body nonadditive potential, even if its shape was precisely fixed.

However, model potentials giving equivalent $J=0$ cross sections will not in general be equivalent if $J>0$ scattering is explored. For instance, Fig. 6 shows the $J=1$ elastic cross sections for ($v=0, j=0$) molecules. Calculations use the same model potentials as the inset of Fig. 4 and can be identified according to the line style. Order of magnitude differences are observed for $J=1$ cross sections in cases where $J=0$ cross sections are identical. One can conclude that the initial characterization of a theoretical model based on purely elastic collisions should take into account a sufficiently broad energy range for the contribution of $J>0$ partial waves to become observable. In alternative, in cases where the method for the production of cold molecules allows the initial rovibrational state to be controlled, at least one experimental inelastic cross section [for some ($v=0, j>0$) initial state, for instance] should complement the elastic collision data.

Please note that one peak is also observed in Fig. 6. Analysis of numerical results based on Eq. (3) shows that $\gamma_r \approx 0.5E_r$, i.e., this feature represents a resonance. The inset shows the resonance width as the peak center is shifted by making the λ parameter vary. Its position below the maximum $\approx 400 \mu\text{K}$ of the $\ell=1$ centrifugal barrier (we find $\gamma_r = E_r$ for $E_r \approx 500 \mu\text{K}$) suggests that it is a shape resonance. However, Feshbach coupling similar to the one found for $J=0$ collisions is not conclusively ruled out.

In conclusion, we have presented a potential-energy surface for $\text{Na}_3(1^4A_2')$. We have demonstrated that long-lived

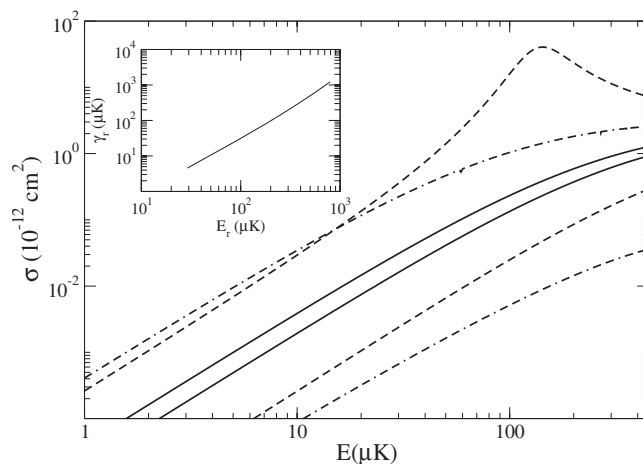


FIG. 6. The partial $J=1$ $\text{Na}+\text{Na}_2$ ($v=0, j=0$) elastic cross section calculated with the same set of model potentials used in the inset of Fig. 4. Same line style is used for corresponding cross sections obtained with the same potential. A resonance can be observed in the upper dashed curve. The inset shows the resonance width γ_r as a function of its position E_r .

triatomic complexes exist and give rise to resonance effects in reactive collisions even at very low collision energies. General features to be expected in atom-molecule scattering in the ultracold regime have also been investigated by performing a systematic variation in the three-body part of the interaction potential. Knowledge of energy-dependent $J=0$ elastic cross sections may not be sufficient to determine the strength of the nonadditive three-body interaction. To this aim, at least one additional $J>0$ elastic or inelastic cross section needs to be experimentally determined. In this work we have studied the sensitivity of scattering observables by introducing a global scaling parameter of the three-body interaction. In perspective, as cold collision empirical data will become available, it is likely that more complex parametrizations of the potential-energy surface will need to be introduced in order to compare quantitatively theory and experiments.

ACKNOWLEDGMENTS

We wish to thank A. Viel for useful discussions. The authors acknowledge support of Egide (PHC Barrande No. 13860UA) and of the Ministry of Education, Youth and Sports of the Czech Republic (KONTAKT project Barrande No. 2-07-3 and Research Project No. 0021620835). P.S. appreciates support of the European Science Foundation and the Czech Science Foundation (EUROCORES program EuroQUAM, project QuDipMol, Grant No. QUA/07/E007).

[1] R. V. Krems, Phys. Chem. Chem. Phys. **10**, 4079 (2008).

[2] J. M. Hutson and P. Soldán, Int. Rev. Phys. Chem. **25**, 497 (2006).

[3] K. M. Jones, E. Tiesinga, P. D. Lett, and P. S. Julienne, Rev. Mod. Phys. **78**, 483 (2006).

[4] T. Köhler, K. Góral, and P. S. Julienne, Rev. Mod. Phys. **78**,

- 1311 (2006).
- [5] S. Jochim, M. Bartenstein, A. Altmeyer, G. Hendl, S. Riedl, C. Chin, J. Hecker Denschlag, and R. Grimm, *Science* **302**, 2101 (2003).
- [6] M. W. Zwierlein, C. A. Stan, C. H. Schunck, S. M. F. Raupach, S. Gupta, Z. Hadzibabic, and W. Ketterle, *Phys. Rev. Lett.* **91**, 250401 (2003).
- [7] M. Greiner, C. A. Regal, and D. S. Jin, *Nature (London)* **426**, 537 (2003).
- [8] J. M. Sage, S. Sainis, T. Bergeman, and D. DeMille, *Phys. Rev. Lett.* **94**, 203001 (2005).
- [9] M. Viteau, A. Chotia, M. Allegrini, N. Bouloufa, O. Dulieu, D. Comparat, and P. Pillet, *Science* **321**, 232 (2008).
- [10] J. G. Danzl, E. Haller, M. Gustavsson, M. J. Mark, R. Hart, N. Bouloufa, O. Dulieu, H. Ritsch, and H.-C. Nägerl, *Science* **321**, 1062 (2008).
- [11] J. Deiglmayr, A. Grochola, M. Repp, K. Mörtilbauer, C. Glück, J. Lange, O. Dulieu, R. Wester, and M. Weidemüller, *Phys. Rev. Lett.* **101**, 133004 (2008).
- [12] F. Lang, K. Winkler, C. Strauss, R. Grimm, and J. Hecker Denschlag, *Phys. Rev. Lett.* **101**, 133005 (2008).
- [13] K.-K. Ni, S. Ospelkaus, M. H. G. de Miranda, A. Pe'er, B. Neyenhuis, J. J. Zirbel, S. Kotochigova, P. S. Julienne, D. S. Jin, and J. Ye, *Science* **322**, 231 (2008).
- [14] J. M. Hutson and P. Soldán, *Int. Rev. Phys. Chem.* **26**, 1 (2007).
- [15] P. Soldán, M. T. Cvitaš, J. M. Hutson, P. Honvault, and J.-M. Launay, *Phys. Rev. Lett.* **89**, 153201 (2002).
- [16] G. Quéméner, P. Honvault, and J.-M. Launay, *Eur. Phys. J. D* **30**, 201 (2004).
- [17] M. T. Cvitaš, P. Soldán, J. M. Hutson, P. Honvault, and J.-M. Launay, *Phys. Rev. Lett.* **94**, 033201 (2005).
- [18] G. Quéméner, P. Honvault, J.-M. Launay, P. Soldán, D. E. Potter, and J. M. Hutson, *Phys. Rev. A* **71**, 032722 (2005).
- [19] G. Quéméner, J.-M. Launay, and P. Honvault, *Phys. Rev. A* **75**, 050701(R) (2007).
- [20] M. T. Cvitaš, P. Soldán, J. M. Hutson, P. Honvault, and J.-M. Launay, *J. Chem. Phys.* **127**, 074302 (2007).
- [21] M. T. Cvitaš, P. Soldán, J. M. Hutson, P. Honvault, and J.-M. Launay, *Phys. Rev. Lett.* **94**, 200402 (2005).
- [22] X. Li, G. A. Parker, P. Brumer, I. Thanopoulos, and M. Shapiro, *J. Chem. Phys.* **128**, 124314 (2008).
- [23] X. Li, G. A. Parker, P. Brumer, I. Thanopoulos, and M. Shapiro, *Phys. Rev. Lett.* **101**, 043003 (2008).
- [24] X. Li and G. A. Parker, *J. Chem. Phys.* **128**, 184113 (2008).
- [25] N. Zahzam, T. Vogt, M. Mudrich, D. Comparat, and P. Pillet, *Phys. Rev. Lett.* **96**, 023202 (2006).
- [26] P. Staunum, S. D. Kraft, J. Lange, R. Wester, and M. Weidemüller, *Phys. Rev. Lett.* **96**, 023201 (2006).
- [27] S. Copping, P. Matei, and B. Stewart, *J. Chem. Phys.* **128**, 241103 (2008).
- [28] P. J. Leo, C. J. Williams, and P. S. Julienne, *Phys. Rev. Lett.* **85**, 2721 (2000).
- [29] A. Marte, T. Volz, J. Schuster, S. Dürr, G. Rempe, E. G. M. van Kempen, and B. J. Verhaar, *Phys. Rev. Lett.* **89**, 283202 (2002).
- [30] A. Simoni, M. Zaccanti, C. D'Errico, M. Fattori, G. Roati, M. Inguscio, and G. Modugno, *Phys. Rev. A* **77**, 052705 (2008).
- [31] A. Simoni and J.-M. Launay, *Laser Phys.* **16**, 707 (2006).
- [32] R. T. Skodje, D. Skouteris, D. E. Manolopoulos, S.-H. Lee, F. Dong, and K. Liu, *Phys. Rev. Lett.* **85**, 1206 (2000).
- [33] P. J. Knowles, C. Hampel, and H.-J. Werner, *J. Chem. Phys.* **99**, 5219 (1993); **112**, 3106(E) (2000).
- [34] J. Čížek, *J. Chem. Phys.* **45**, 4256 (1966).
- [35] The Na valence basis set (12s, 12p, 5d, 2f, 1g) used for sodium consisted of one (13s)→[1s] contracted function and (11s12p5d2f1g) uncontracted Gaussian type basis functions with exponents determined in an even-tempered manner: for s 11 exponents with center 1.0 and ratio 2.1, for p seven exponents with center 3.0 and ratio 2.5 and five exponents with center 0.02 and ratio 2.5, for d five exponents with center 0.1 and ratio 2.8, for f two exponents with center 0.125 and ratio 3.0, and for g one exponent 0.1.
- [36] J. Higgins, T. Hollebeek, J. Reho, T.-S. Ho, K. K. Lehmann, H. Rabitz, G. Scoles, and M. Gutowski, *J. Chem. Phys.* **112**, 5751 (2000).
- [37] P. Soldán, M. T. Cvitaš, and J. M. Hutson, *Phys. Rev. A* **67**, 054702 (2003).
- [38] J. Kłos, P. S. Żuchowski, Ł. Rajchel, G. Chałasiński, and M. M. Szczesniak, *J. Chem. Phys.* **129**, 134302 (2008).
- [39] S. F. Boys and F. Bernardi, *Mol. Phys.* **19**, 553 (1970).
- [40] MOLPRO is a package of *ab initio* programs written by H.-J. Werner and P. J. Knowles with contributions from others; for more information see <http://www.tc.bham.ac.uk/molpro/>.
- [41] T.-S. Ho and H. Rabitz, *J. Chem. Phys.* **104**, 2584 (1996).
- [42] M. Gutowski, *J. Chem. Phys.* **110**, 4695 (1999).
- [43] V. S. Ivanov, V. B. Sovkov, and L. Li, *J. Chem. Phys.* **118**, 8242 (2003).
- [44] T.-S. Ho and H. Rabitz, *J. Chem. Phys.* **113**, 3960 (2000).
- [45] J. Mitroy and M. W. J. Bromley, *Phys. Rev. A* **68**, 052714 (2003).
- [46] P. Soldán and J. M. Hutson, *J. Chem. Phys.* **112**, 4415 (2000).
- [47] F. A. van Abeelen and B. J. Verhaar, *Phys. Rev. A* **59**, 578 (1999).
- [48] F. H. Mies, E. Tiesinga, and P. S. Julienne, *Phys. Rev. A* **61**, 022721 (2000).
- [49] C. Samuelis, E. Tiesinga, T. Laue, M. Elbs, H. Knöckel, and E. Tiemann, *Phys. Rev. A* **63**, 012710 (2000).
- [50] M. T. Cvitaš, P. Soldán, and J. M. Hutson, *Mol. Phys.* **104**, 23 (2006).
- [51] B. M. Axilrod and E. Teller, *J. Chem. Phys.* **11**, 299 (1943); Y. Muto, *Proc. Phys. Math. Soc. Jpn.* **17**, 629 (1943).
- [52] R. J. Bell, *J. Phys. B* **3**, 751 (1970).
- [53] S. H. Patil and K. T. Tang, *J. Chem. Phys.* **106**, 2298 (1997).
- [54] W. L. Bade, *J. Chem. Phys.* **28**, 282 (1958).
- [55] J.-M. Launay and M. Le Dourneuf, *Chem. Phys. Lett.* **169**, 473 (1990).
- [56] N. F. Mott and H. S. W. Massey, *The Theory of Atomic Collisions* (Oxford University Press, Oxford, 1965).
- [57] F. H. Mies, E. Tiesinga, and P. S. Julienne, *Phys. Rev. A* **61**, 022721 (2000).
- [58] E. P. Wigner, *Phys. Rev.* **98**, 145 (1955).
- [59] V. Aquilanti, S. Cavalli, A. Simoni, A. Aguilar, J. M. Lucas, and D. De Fazio, *J. Chem. Phys.* **121**, 11675 (2004).
- [60] A. Simoni, P. S. Julienne, E. Tiesinga, and C. J. Williams, *Phys. Rev. A* **66**, 063406 (2002).